Chen *et al. Virology Journal* (2023) 20:81
https://doi.org/10.1186/s12985-023-02036-9

Virology Journal

RESEARCH Open Access

Isolation and characterization of a novel phage belonging to a new genus against *Vibrio parahaemolyticus*

Yubing Chen[1,2], Wenqing Li[1,3], Keming Shi[1,3], Zheng Fang[2], Yunlan Yang[1,3*] and Rui Zhang[4*]

Abstract

Background *Vibrio parahaemolyticus* is a major foodborne pathogen that contaminates aquatic products and causes great economic losses to aquaculture. Because of the emergence of multidrug-resistant *V. parahaemolyticus* strains, bacteriophages are considered promising agents for their biocontrol as an alternative or supplement to antibiotics. In this study, a lytic vibriophage, vB_VpaM_R16F (R16F), infecting *V. parahaemolyticus* 1.1997^{T} was isolated, characterized and evaluated for its biocontrol potential.

Methods A vibriophage R16F was isolated from sewage from a seafood market with the double-layer agar method. R16F was studied by transmission electron microscopy, host range, sensitivity of phage particles to chloroform, one-step growth curve and lytic activity. The phage genome was sequenced and in-depth characterized, including phylogenetic and taxonomic analysis.

Results R16F belongs to the myovirus morphotype and infects *V. parahaemolyticus*, but not nine other *Vibrio* spp. As characterized by determining its host range, one-step growth curve, and lytic activity, phage R16F was found to highly effective in lysing host cells with a short latent period (< 10 min) and a small burst size (13 plaque-forming units). R16F has a linear double-stranded DNA with genome size 139,011 bp and a G + C content of 35.21%. Phylogenetic and intergenomic nucleotide sequence similarity analysis revealed that R16F is distinct from currently known vibriophages and belongs to a novel genus. Several genes (e.g., encoding ultraviolet damage endonuclease and endolysin) that may enhance environmental competitiveness were found in the genome of R16F, while no antibiotic resistance- or virulence factor-related gene was detected.

Conclusions In consideration of its biological and genetic properties, this newly discovered phage R16F belongs to a novel genus and may be a potential alternate biocontrol agent.

Keywords *Vibrio parahaemolyticus*, Vibriophage, Biological features, Genomic analysis, Phage therapy

*Correspondence:
Yunlan Yang
yangyunlan@xmu.edu.cn
Rui Zhang
ruizhang@szu.edu.cn
[1]State Key Laboratory of Marine Environmental Science, Xiamen University, Xiamen 361102, Fujian, China
[2]China-ASEAN College of Marine Sciences, Xiamen University Malaysia, Sepang 43900, Selangor, Malaysia
[3]College of Ocean and Earth Sciences, Fujian Key Laboratory of Marine Carbon Sequestration, Xiamen University, Xiamen 361102, Fujian, China
[4]Institute for Advanced Study, Shenzhen University, Shenzhen 518061, Guangdong, China

Background

Vibriosis is one of the most prevalent bacterial diseases that causes mortality of shrimp, fish and shellfish. It results from contamination with *Vibrio* pathogens, such as *V. parahaemolyticus*, *V. vulnificus*, *V. alginolyticus* and *V. harveyi* [1, 2]. With the rapid development of aquaculture and the rise in consumption of aquatic products, vibriosis in global aquaculture and *Vibrio*-related food poisoning cases are increasing [1, 3, 4]. *V. parahaemolyticus* is ubiquitous in seawater and seafood-associated environments [5–7]. According to a comprehensive review and meta-analysis of studies between 2003 and 2015 on the occurrence and prevalence of *V. parahaemolyticus* in seafood, it could be isolated from 47.5% of all seafood samples, and showed high overall prevalence rates in oysters (63.4%), clams (52.9%), fish (51.0%), shrimps (48.3%), and mussels, scallop and periwinkle (28.0%) [8]. Eating any raw *V. parahaemolyticus*-contaminated seafood can lead to gastroenteritis because the pathogen contains various virulence factors, including adhesin, heat-resistant direct hemolysin (TDH), TDH-associated hemolysin, and the type III secretory system [9]. The reported incidence of *V. parahaemolyticus* in fishery products in China was approximately 15% during the period 2008 to 2017 [10]. The administration of antibiotics to quickly and effectively control pathogenic *Vibrio* strains became common in aquaculture. However, prolonged use of antibiotics has resulted in an increase in the number of multidrug-resistant *Vibrio* strains, presenting a substantial threat to the control of vibriosis [11–13]. Calls have been made to decrease antibiotic use, and alternative measures to control bacterial pathogens are urgently required.

Phages infect and lyse host bacterial cells and plunder host cell resources for their own reproduction [14–17]. Phages have been known as a potential antibacterial agent for over a century; they were used against human bacterial infection in the 1920s [18]. Previous studies have reported on global efforts to prevent and control *Vibrio* in aquaculture by using phages. Numerous in vitro and in vivo studies have shown that phage therapy was effective in controlling vibriosis caused by *Vibrio* (e.g., *V. parahaemolyticus* and *V. harveyi*) in shrimp, sea cucumber, abalone, oysters, and other species [19–23]. By way of illustration, a 78.1% reduction in bacterial counts was observed within 1 h of phage application during an efficacy study of phage against *V. parahaemolyticus* in shrimp [23]. *V. parahaemolyticus*-infected shrimp larvae regained activity with no significant reduction in survival when they were treated with phage [20]. The application of phages in a variety of aquaculture situations highlights the potential of phage therapy to decrease bacterial infections and diminish the significant economic losses to aquaculture and the harm to public health caused by contamination with *Vibrio*.

The selection of appropriate phages is, however, a prerequisite, and important tests need to be performed before phage therapy can be applied in the field. In this study, a novel bacteriophage that infects *V. parahaemolyticus* 1.1997^{T} was isolated from sewage from the Chigang seafood market in Guangdong, China. The phage was characterized based on morphological, host specificity, life cycle, genomic character and taxonomy, and evaluated for its bactericidal ability and possible use in phage therapy.

Methods

Phage isolation and purification

V. parahaemolyticus 1.1997^{T} brought from Guangdong marine pathogenic *Vibrio* company in China was used as the host bacterium for phage isolation. It was incubated in rich organic (RO) medium (1 M peptone, 1 M yeast extract, and 1 M sodium acetate in artificial seawater, pH 7.5) at 30℃ with a shaking speed of 160 rpm min^{-1} [24]. The sewage samples used for phage isolation were collected from the seafood markets in Guangzhou, China (23.10°N, 113.33°E), and filtered through a 0.22-μm membrane (Millipore, Massachusetts, USA) to remove bacteria and large particles. The sewage samples were added into an exponentially growing host bacterial culture to allow plaque formation using the double-layer agar method [25]. A clear individual plaque was collected and suspended in storage medium (SM; 8 mM $MgSO_4$, 50 mM Tris-HCl, and 100 mM NaCl, pH 7.5). After purifying at least five times, the well-separated plaque was collected and stored in SM at 4 °C.

Phage amplification and enrichment

To obtain high-titer phage suspension, a purified phage plaque was inoculated into bacterial culture and amplified overnight, followed by centrifugation at 12,000 × *g* for 10 min. The supernatant was filtered through a 0.22-μm membrane to remove cell fragments. The filtrate was precipitated with polyethylene glycol 8000 (10% w/v) overnight. Then, phage pellets were obtained through centrifugation (10,000 × *g*, 60 min, 4 °C) and resuspended in SM. The phage particles were subjected to cesium chloride solutions (ρ=1.3, 1.5, 1.7 g mL^{-1}) for purification and centrifuged at 200,000 × *g* at 4 °C for 24 h using an Optima L-100 XP ultracentrifuge (Beckman Coulter, CA, USA). The purified phage particles were dialyzed through 30-kDa superfilters (Millipore, Bedford, MA, USA).

Transmission electron microscopy (TEM)

Phage morphology was characterized by TEM. Briefly, approximately 20 μL of phage suspension was added onto

the surface of a copper grid to adsorb in darkness for 30 min. Then, the phage sample was negatively stained with phosphotungstic acid (1%, pH 7.0) for 20 min and dried for 30 min. The phage sample was examined using a JEM-2100 transmission electron microscope (JEOL, Tokyo, Japan).

Determination of the host range

A total of 35 *Vibrio* strains, including 6 strains of *V. parahaemolyticus* and 29 strains of other species (*V. alginolyticus*, *V. antiquarius*, *V. azureus*, *V. campbellii*, *V. caribbeanicus*, *V. chagasii*, *V. cholerae*, *V. fortis*, *V. harveyi*, *V. inhibens*, *V. neocaledonicus*, *V. owensii*, *V. rotiferianus*, *V. tubiashii*, *V. variabilis* and *V. xuii*), were used to determine the lytic host range of the phage isolated in this study with the double-layer agar method (Table S1). The bacteria strains were grown on the RO agar medium plates and single colony was collected and then incubated in RO liquid medium at 30℃ with a shaking speed of 160 rpm min^{-1}. The log-phase bacteria strains (incubated about 2–10 h) were mixed with the phage and kept in the dark for 20–30 min for infection. After infection, the phage-host mixtures were added with molten RO agar medium and poured onto solid agar plates, then incubated overnight at 28 °C. All bacteria strains have been tested at least three times. The presence of plaques on a bacterial lawn was checked to determine phage infection of the host bacterium.

Lipid test

To investigate whether the phage capsids contain lipid, phages were mixed with 0%, 0.2%, 2% or 20% chloroform and incubated in darkness at room temperature for 30 min. Then, the mixtures were centrifuged at 12,000 × *g* for 5 min and the phages were obtained from the upper suspension. The chloroform sensitivity of the phages was determined by the presence or absence of plaques on double-layer agar. The lipid test was carried out twice.

One-step growth curve

A one-step growth curve was determined to study the infectivity and replication ability of the phage. Briefly, phages were added to an early log-phase host culture (*V. parahaemolyticus* 1.1997^{T}) at a multiplicity of infection of 0.03 and incubated for 20 min at room temperature in the dark. Then, phages that were not adsorbed were removed by centrifugation (8,000 × *g*, 4 °C, 5 min), and the cell pellets were washed and resuspended in 100 mL of RO medium. The phage suspension was incubated at 28 °C with a shaking of 160 rpm min^{-1}. Subsamples were obtained at 10-min intervals and assayed by the double-layer agar method. The burst size was calculated as the ratio between the number of phages before and after the burst [26]. The experiment of one-step growth curve has been conducted with three replications.

Determination of lytic activity

To understand the efficiency of bacterial inactivation, a lytic activity for the phage against *V. parahaemolyticus* were assessed at different multiplicity of infections (MOIs) by monitoring the OD_{600} (optical density measurements at a wave-length of 600 nm) using a microplate reader (Synergy H1, Bio-Tek, USA). Briefly, freshly prepared host culture was added to the a 96-well plate before infection with high-titer phage suspension at various MOIs (0.001, 0.01, 0.1, 1 and 10). Wells inoculated with RO medium or *V. parahaemolyticus* only was served as control groups. The plate was placed in the instrument and incubated at 30℃ with orbital shaking. The OD_{600} of the cultures were monitored in real time and recorded every 30 min. The assay was conducted with eight replications for each treatment.

DNA extraction and phage genome sequencing

Phage DNA was obtained by using the phenol–chloroform extraction method. Briefly, approximately 1 mL of high-titer phage suspension was treated with proteinase K, sodium dodecyl sulfate (10% w/v), and ethylenediaminetetraacetic acid (EDTA; pH 8.0) and incubated at 55 °C for 3 h. The digested sample was purified with phenol/chloroform/isoamyl alcohol (25:24:1 v:v:v) and chloroform/isoamyl alcohol (24:1 v:v) to remove any debris. Next, the DNA pellet was washed with pre-cooled 70% ethanol, air-dried at room temperature, dissolved in Tris-EDTA buffer (10 mM Tris-HCl, 1 mM EDTA, pH 8.0), and stored at 4 °C. The phage genome was sequenced and assembled using the Illumina HiSeq 4000 platform with a 150-bp paired-end DNA library and Velvet software (v.1.2.03) [27].

Genome annotation

The phage termini and packaging mechanism were identified by the online service PhageTerm on a Galaxy-based server (https://galaxy.pasteur.fr) [28]. The GeneMarkS online server (http://topaz.gatech.edu/GeneMark/genemarks.cgi) was used to identify putative open reading frames (ORFs) [29]. The functions of ORFs were annotated by BLASTP online against the non-redundant (nr) database of the National Center for Biotechnology Information (NCBI), with a cut-off *e*-value of $<10^{-5}$, and the results were checked manually. Putative transfer RNA (tRNA) genes were detected with tRNAscan-SE (http://lowelab.ucsc.edu/tRNAscan-SE/) [30]. Virulence factors and antibiotic resistance-encoding genes were searched using the Virulence Factor Database (VFDB, http://www.mgc.ac.cn/VFs/main.htm) and the Comprehensive Antibiotic Resistance Database (CARD, https://

card.mcmaster.ca/analyze/rgi) webservers, respectively [31, 32]. In addition, genome-based life cycle classification was also carried out using an online platform called PhageAI (https://phage.ai/). The complete genome data was deposited in the GenBank database with accession number OP793884.

Phylogenetic and taxonomic analysis

Viral CONTigs Automatic Clustering and Taxonomy v.2.0 (vConTACT2) was used to compare the isolated phage against the Prokaryotic Viral RefSeq 207 database using whole genome gene-sharing profiles, and related phages were identified by genome pairs with a similarity score>1 [33]. The whole phage sequence was also submitted to NCBI BLASTN to search forsimilar sequences. To analyze the evolutionary relationships of the phage, complete amino acid profiles of phages were submitted to the Virus Classification and Tree Building Online Resource (VICTOR, https://ggdc.dsmz.de/victor.php) for phylogenetic tree construction [34, 35]. All pairwise comparisons of the amino acid sequences were conducted using the Genome-BLAST Distance Phylogeny (GBDP) method with the settings recommended for prokaryotic viruses [34, 36]. Branch support was inferred from 100 pseudo-bootstrap replicates each, and the tree was rooted at the midpoint and visualized with ggtree [37, 38]. In addition, intergenomic nucleotide sequence similarity and aligned genome fractions within the imported phages were plotted with the Virus Intergenomic Distance Calculator (VIRIDIC) using default parameters [39].

Results and discussion

Biological properties of phage R16F

Vibriophage vB_VpaM_R16F (hereafter R16F) was isolated from a sewage sample from Chigang seafood market, Guangzhou, China, by infecting *V. parahaemolyticus* 1.1997^{T}. R16F formed clear plaques around 2–3 mm in diameter after infection for 12 h (Fig. 1A). With extension of the incubation time, the phage plaques became larger (up to 7–8 mm in diameter) with a turbid halo on the host bacterial lawn (Fig. 1A). Halo formation has previously been described as an indicator of phage-associated exopolysaccharide depolymerization [40, 41]. The depolymerases encoded by phages can specifically cleave polysaccharides (e.g. capsular polysaccharides, exopolysaccharides or lipopolysaccharides) of the host bacteria and therefore provide a significant advantage for phages to adsorb onto their hosts [42, 43]. Such halo zones have been observed for various phages, including phages that infect *Pseudomonas putida*, *Klebsiella pneumoniae*, and *V. alginolyticus* [44–46]. TEM revealed that R16F has a narrow neck or collar region, an icosahedral capsid (head diameter 83±7 nm), and a complete tail with contracted sheath (49±2–100±3 nm). It belongs to the myovirus morphotype (Fig. 1B).

To further understand the lytic cycle of R16F, a one-step growth curve was constructed, which showed a short latent period for R16F, less than 10 min (Fig. 1C). The latent period is the minimum time it takes from phage adsorption to lysis of the host with the release of progeny virions. The burst size for R16F, defined as the average number of progeny virions liberated by one infected host cell at the completion of a growth cycle, estimated from the one-step growth curve, was 13 plaque-forming units (PFU) $cell^{-1}$ (Fig. 1C). Short latent periods (<30 min) and small burst sizes (ranging from 10 to 100 PFU $cell^{-1}$) have been observed for other phages that infect *V. parahaemolyticus* [7, 10, 47–54]. A trade-off between burst size and latent period has been reported in lytic phage generation because phages are released from infected cells at the cost of destruction of the machinery necessary to produce more phage progeny [55]. Thus, phages with short latent periods at the cost of their burst size may be viewed as specialists for propagation when bacteria are prevalent.

R16F exhibited a narrow lytic spectrum and only infected the original host *V. parahaemolyticus* 1.1997^{T} among the species tested (Table S1). R16F was insensitive to chloroform, suggesting that there was no lipid in the viral capsid. This result was consistent with the previous suggestion that lipids are rare among phages, occurring in <4% of isolates [56].

Given that the efficiency of the phage in bacterial inactivation is one of the critical properties should be considered for potential candidates in phage therapy, lytic activity analysis of R16F was tested in this study. The killing curves showed that R16F was highly effective against *V. parahaemolyticus* 1.1997^{T} at all MOIs tested (Fig. 2). Moreover, in these samples, there was no observable difference in inhibitory effects after 10 h of incubation, even at the lowest MOI (MOI=0.001). R16F exhibited inhibition of bacterial growth regardless of the value of the MOIs, suggesting that increasing phage loads would lead to a limited positive effect on host inactivation of the phage with strong lytic ability. Although few phages were applied in bacteria inhibition, *V. parahaemolyticus* 1.1997^{T} could still be lysed by R16F within a short time which might benefit from the short latent of the phage.

Overview of genomic features and taxonomy of R16F

Whole genome sequencing revealed that the R16F genome is a 139,011-bp linear double-stranded DNA with a G+C content of 35.21%, which is lower than its host (45.3%). According to the results from PhageTerm, a fixed position was recognized on the DNA of R16F and 353-bp direct terminal repeats (DTR) were observed, suggesting that the DNA termini of R16F belong to the

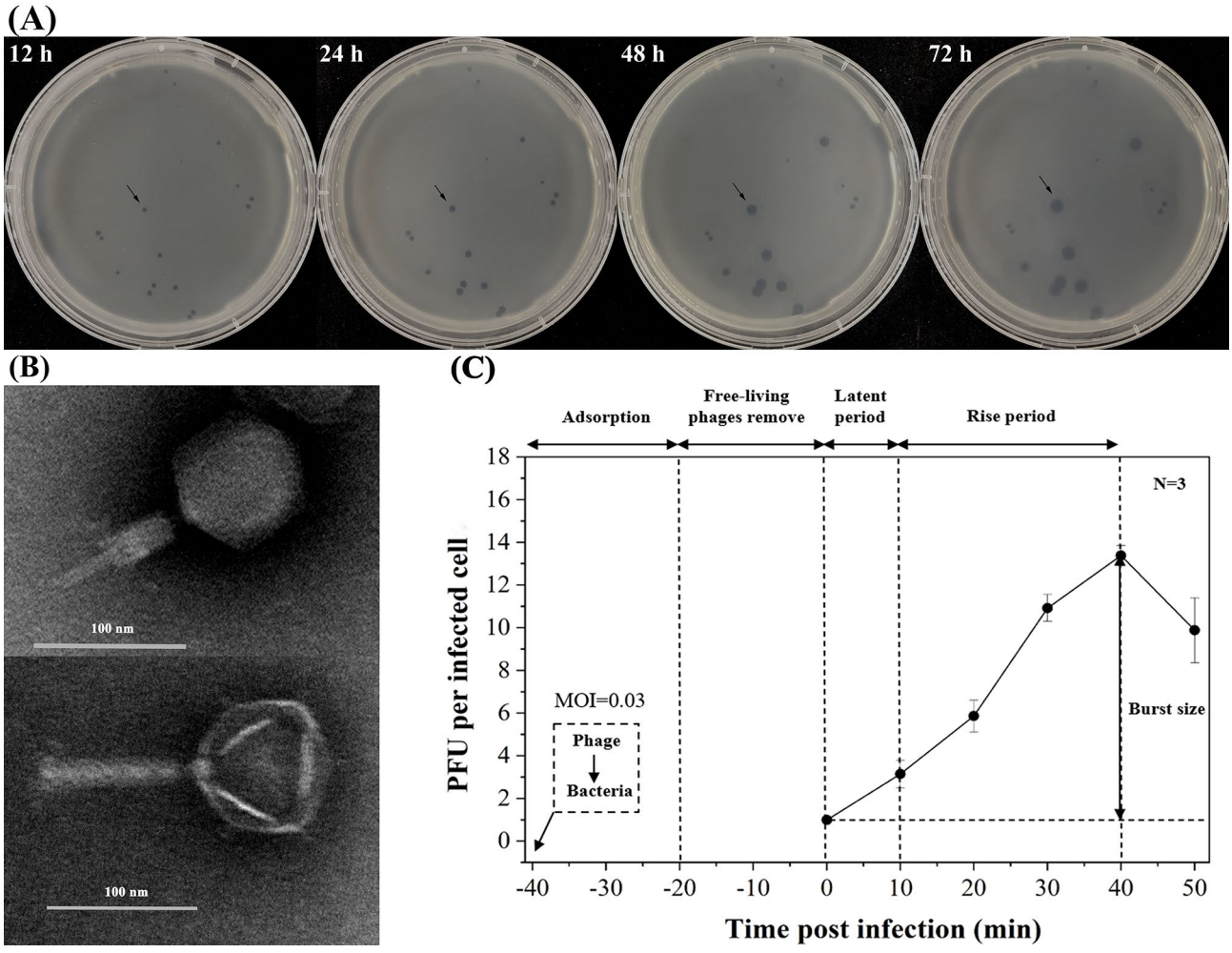

Fig. 1 Morphology and infection dynamics of vibriophage vB_VpaM_R16F (R16F). (**A**) The plaque morphology of R16F after incubation with *V. parahaemolyticus* 1.1997^{T} for 12, 24, 48 and 72 h. The phage plaques are surrounded by expanding opaque haloes as the incubation time is extended. (**B**) Transmission electron micrographs of R16F with contracted tail (upper panel) and non-contracted tail (lower panel). (**C**) One-step growth curve of R16F. Phages were incubated with an early log-phase *V. parahaemolyticus* 1.1997^{T} at a multiplicity of infection of 0.03. PFU, plaque-forming units. The given values are the average of three determinations (N = 3)

DTR class. A total of 260 ORFs were identified in the genome of R16F, of which only 57 (21.92%) have known functional domains, while the remaining 203 (70.77%) were annotated as hypothetical proteins (Fig. 3; Table S2). The functional ORFs were identified to encode proteins that can be arranged in functional categories including phage structural formation, genome packaging, nucleotide metabolism, integration, lysis, and other functions. Among these functional ORFs, about 12.69% (33/260) are conserved. The genome of R16F was predicted to encode two tRNAs ($tRNA^{Arg}$ and $tRNA^{Met}$) carried anticodons TCT (serine) and CAT (histidine). No antibiotic resistance- or virulence factor-related gene was found in the genome of R16F.

On the basis of NCBI BLASTN analysis, phages qdvp001, VPMCC14, and PWH3a-P1 share the highest sequence identities (95.15%, 84.98%, and 88.33%, respectively) with R16F, but they share only 33%, 15%, and 12% query coverage. To investigate the evolutionary relationships and taxonomic status of R16F, the vConTACT2 database was used to detect other homologous phages. A total of 37 phages with a similarity score of >1 were identified, including six vibriophages with high scores of >40 (Table S3). All the phages detected by vConTACT2 and other phage sequences obtained from NCBI BLASTN were used to construct a phylogenetic tree based on pairwise comparisons of the amino acid sequences of R16F. According to the phylogenetic analysis, R16F was most closely related to vibriophage qdvp001 with only 67% pairwise sequence identity (Fig. 4A). To better estimate the similarity between phage genomes, all phages from the tree were imported into the VIRIDIC software and demarcated based on the default similarity thresholds of 95% for species and 70% for genus [39,

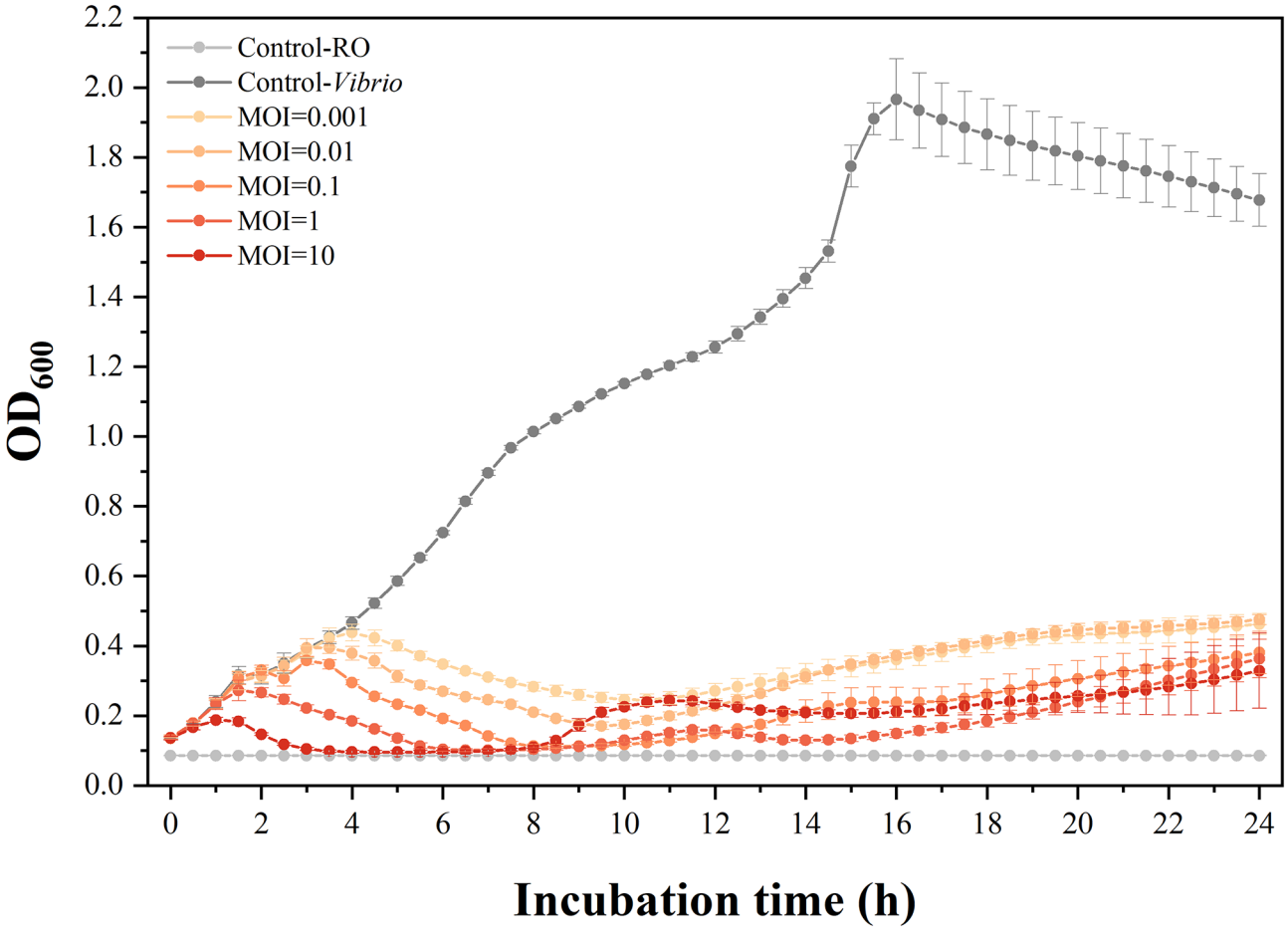

Fig. 2 Lytic activity of R16F at various multiplicities of infection (MOIs) against *V. parahaemolyticus* 1.1997^{T}. Five different MOIs (0.001, 0.01, 0.1, 1 and 10) were used for infecting *V. parahaemolyticus* 1.1997^{T}. The dark grey graph shows a standard growth curve of *V. parahaemolyticus* 1.1997^{T} in solution (i.e., the negative control). The light grey represents RO solution as a mock control. The given values are the average of eight determinations (N = 8)

57]. The VIRIDIC results showed that the highest value of intergenomic similarity was only 34.9%, observed between R16F and qdvp001 (Fig. 4B). Therefore, R16F is suggested to belong to a novel genus. Overall, R16F is considered a novel phage with a genome that differs from all previously described phage sequences.

DNA repair genes in the genome of phage R16F

Phage R16F harbors a gene (ORF 21) encoding an ultraviolet damage endonuclease (UVDE), which is involved in DNA repair. UV light may cause damage or mortality to bacteria and phages [58]. In bacterial cells, UVDE has been defined as a repair protein that is capable of identifying and removing various DNA lesions including UV photoproducts as well as non-UV-induced DNA damage such as a basic sites, strand breaks, and gaps [59]. In addition to being found in the genomes of bacteria and fungi, UVDE is present in the genomes of some phages [60, 61]. UVDE of bacteriophage T4 was involved in the dark repair of UV light damage in T4-infected cells [62]. Furthermore, a conserved catalytic GIY-YIG domain of nucleotide excision repair endonucleases UvrC, Cho, and similar proteins, is encoded in the R16F genome (ORF 31). UvrA, UvrB, and UvrC mediate nucleotide excision repair following various types of structurally unrelated DNA damage and remove the complete oligonucleotide containing the damage [63–67].

Type II toxin-antitoxin (TA) system HicB family antitoxin gene

A gene (ORF 24) encoding a type II TA system HicB family antitoxin (HicB) was found in the genome of R16F. TA systems are composed of a two-gene cassette encoding a toxic protein and an antitoxin protein, the latter counteracting the toxicity of the former [68]. Type II TA systems appear to be the most abundant and diverse in bacterial and archaeal genomes, largely being found in mobile gene modules such as plasmids and phages, but also in bacterial chromosomes, and they are highly prone to horizontal gene transfer [68–70]. Type II TA systems in bacteria are thought to be involved in diverse biological processes, including plasmid maintenance, phage inhibition,

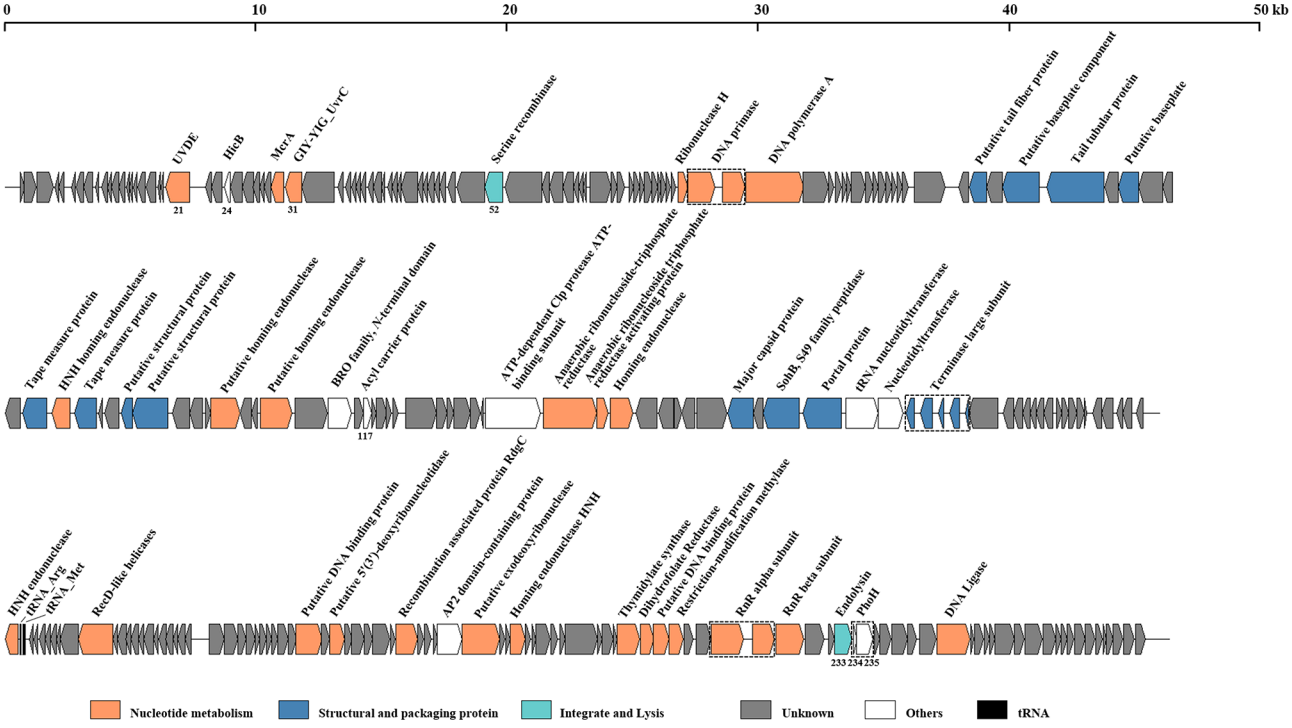

Fig. 3 Genomic organization of R16F. Putative open reading frames are represented by arrows and were classified into different functional categories indicated by the colors shown at the bottom of the figure. UVDE, putative UV DNA damage repair endonuclease; HicB, type II toxin–antitoxin system HicB family antitoxin; McrA, 5-methylcytosine-specific restriction endonuclease; GIY-YIG UvrC, catalytic GIY-YIG domain of nucleotide excision repair endonucleases UvrC, Cho, and similar proteins; PhoH, phosphate starvation-inducible protein

persistence, stress response, and biofilm formation [68, 71]. The hicAB system, a type II TA system, encoding toxin HicA and antitoxin HicB proteins, has been predicted to be associated with several functions, including RNA-binding, persister cell formation and involvement in extracytoplasmic stress responses [69, 72, 73]. On the basis of BLASTP analysis, almost all homologues of the HicB in R16F were from bacterial genomes, implying that the HicB in R16F most likely derived from bacteria via horizontal gene transfer. However, no gene encoding a HicA toxin protein was identified in R16F. Hitherto, intact TA systems have been found in prophages, such as prophages induced from *Streptococcus suis*, *Mannheimia haemolytica* and *Acinetobacter*. However, this is the first report of a component of a TA system in a lytic phage [74–76]. A recent review suggested that phages have evolved defenses against TA systems by incorporating active TA systems [77]. The roles of TA systems in phage genomes, especially those of lytic phages, remain unclear, but they are speculated to perform functions in phage–bacteria co-evolution.

Acyl carrier protein (ACP)

ACP (ORF 117 in phage R16F) serves as a ubiquitous and highly conserved transporter of acyl intermediates during the synthesis of fatty acids [78]. ACPs in bacteria are acyl donors for synthesis of various products, including endotoxin and acylated homoserine lactones, which are involved in quorum sensing. The unique nature of these growth and pathogenesis processes makes ACP-dependent enzymes a target for antibacterial agents [78]. In addition to being widespread in bacteria, homologs of ACP have been identified in several phages, such as *V. helene* phage 12B3, *Erythrobacter* phage vB_EliS-R6L, and some prophages [79, 80]. ACP encoded by phages was previously identified as an auxiliary metabolic gene and potentially involved in the biosynthesis of secondary metabolites in host cells [80].

Phosphate starvation-inducible protein (phoH)

The genome of phage R16F also harbors a phoH gene (ORFs 234 and 235). In *Escherichia coli*, gene transcription of the phosphate regulator is activated in response to phosphate restriction, and its products participate in the transportation and use of various forms of phosphate [81–83]. The phoH gene has been detected in marine phages, including vibriophages, cyanophages, and roseophages [24, 84–87]. Although many studies have hypothesized that phage-encoded phoH might play an important role in assisting host phosphorous metabolism, no concrete evidence has been reported to support this conjecture.

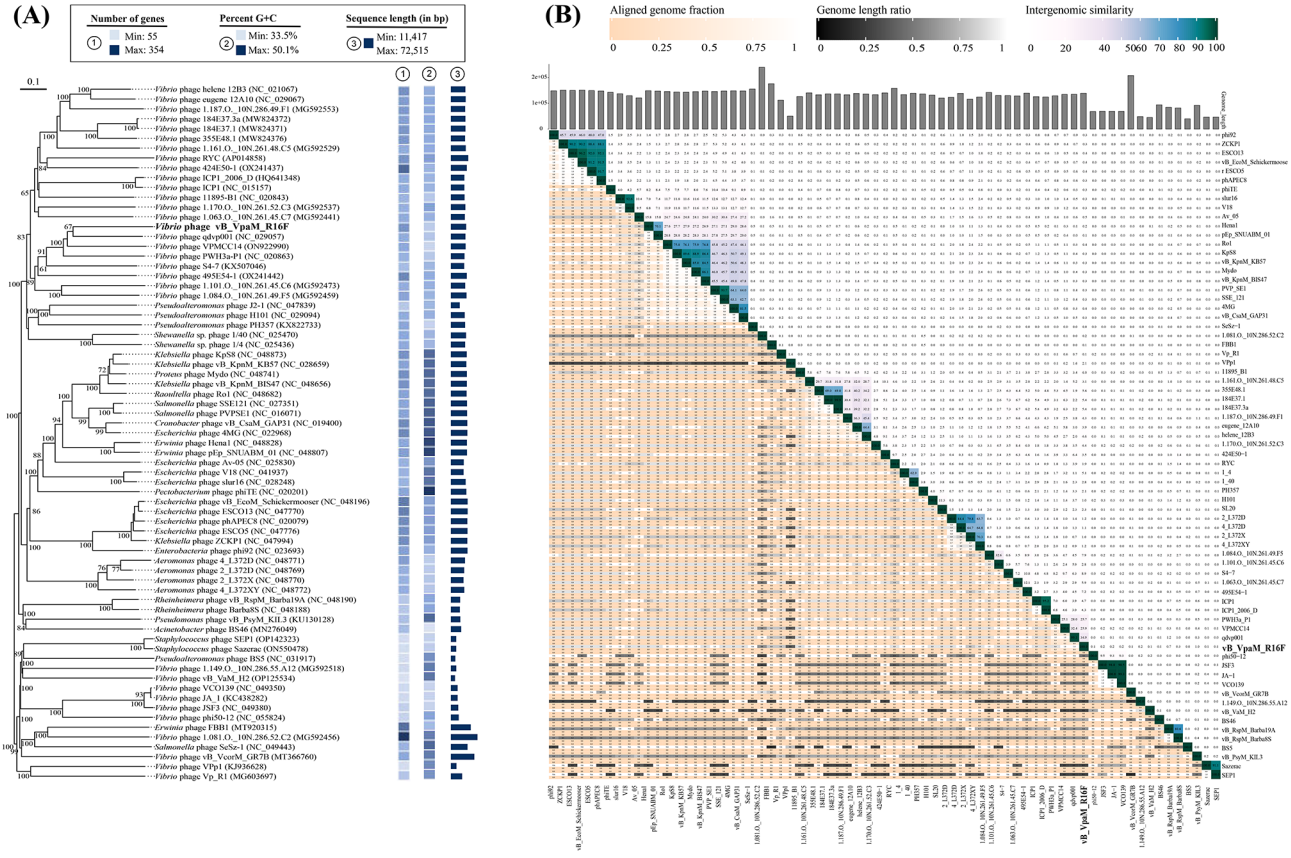

Fig. 4 Taxonomy of R16F. (**A**) Phylogenetic tree, including R16F and other closely related phages, constructed using the Virus Classification and Tree Building Online Resource (VICTOR) web service. Pairwise comparisons of the amino acid sequences were conducted using the Genome-BLAST Distance Phylogeny (GBDP) method with settings recommended for prokaryotic viruses. The numbers above branches are GBDP pseudo-bootstrap support values from 100 replications. (**B**) Virus Inter-genomic Distance Calculator (VIRIDIC)-generated heatmap incorporating intergenomic similarity values (right half) and alignment indicators (left half and top annotation)

Phage therapy potential inferred from biological and genomic features of R16F

The biological and genomic characteristics are critical in evaluating phage fitness and identifying candidates for use in phage therapy. Several general properties should be considered, including bactericidal ability, efficiency, and whether the phage carries endotoxins [88]. Phages have often evolved to quickly suppress bacterial proliferation when the bacterial density is sufficiently high [55]. This phenomenon was observed here for R16F (latent period < 10 min, with small burst size). Moreover, the efficiency of bacterial inactivation was evaluated in various MOIs. Our findings demonstrated that R16F has highly effective inactivation in the prevention and control of *V. parahaemolyticus*. Therefore, R16F with strong lytic ability may be effective against *Vibrio* outbreaks in a short time. The narrow lytic spectrum (host range) of R16F would enable use of this phage to specifically target *V. parahaemolyticus*. Moreover, previous study suggested that various type of phage with narrow host specificity can be mixed in cocktails to control a range of pathogenic strains [48].

R16F was found to encode an endolysin (ORF 233) that produced at the later stage of phage replication and would be able to hydrolyze the bacterial peptidoglycan layer of the host cell wall from within, leading lysis of the host bacterium and release newly assembled phage particles [89]. In recent studies, phage-encoded endolysin are believed to have good performance to control foodborne pathogens including gram-negative bacteria and remove bacterial biofilms [42, 90]. The R16F-encoded endolysin showed 95.76% amino acid sequence identity with the endolysin encoded by phage qdvp001 (lysqdvp001). Lysqdvp001 and its homologues are highly divergent enzymes with superior lytic activity and a broader spectrum than their parent phages [51, 91]. Therefore, we infer that both vibriophage R16F and R16F-derived endolysin are promising for application in biocontrol.

No antibiotic resistance- or virulence factor-related gene was predicted in the genome of R16F using VFDB and CARD, indicating that R16F infection is unlikely to result in enhancement of *Vibrio* virulence or contamination of aquaculture environments with antibiotic resistance genes. Although R16F encodes a serine

recombinase (ORF 52), no attachment sites on the phage or bacterial genomes (*attP–attB*) were observed in the 1000-nt sequences adjacent to either end of the serine recombinase-encoding gene. In addition, a PhageAI analysis revealed that the probability of phage R16F being virulent was found to be 91.53%. Therefore, R16F is considered safe at the genetic level as a biocontrol agent.

Conclusions

This study isolated a lytic phage, vB_VpaM_R16F (R16F), active against *Vibrio parahaemolyticus* 1.1997^{T} and investigated its biological properties. R16F is a myovirus with an icosahedral head and a contracted tail. R16F exhibits a narrow host spectrum, highly effective lytic activity, small burst size, and short latent period. A large portion of the genes of R16F are annotated as hypothetical proteins. However, serval functional genes that may improve the environmental competitiveness of the phage were found in the genome of R16F. Antibiotic resistance or virulence factor-related genes were not detected. R16F was most closely related to vibriophage qdvp001 with only 67% pairwise sequence identity and the highest value of intergenomic similarity was only 34.9%. R16F is considered a newly described vibriophage with a genome that differs from all previously described, belonging to a novel genus. The biological and genetic properties suggest that R16F has the potential to be used as a biocontrol agent for vibriosis induced by *V. parahaemolyticus*. However, further experiments still need to be conducted in the future to investigate the potential of R16F as a biological reagent for phage therapy, specifically with regards to lysogenic testing, pH and temperature stabilities, and so on. These follow-up studies will provide a deeper understanding of the practical applications of R16F in combating vibriosis caused by *V. parahaemolyticus*.

List of abbreviations

ACP	acyl carrier protein
CARD	Comprehensive Antibiotic Resistance Database
CAT	histidine
DTR	direct terminal repeats
EDTA	ethylenediaminetetraacetic acid
GBDP	Genome-BLAST Distance Phylogeny
GIY-YIG UvrC	catalytic GIY-YIG domain of nucleotide excision repair endonucleases UvrC, Cho, and similar proteins
HicB	HicB family antitoxin
McrA	5-methylcytosine-specific restriction endonuclease
NCBI	National Center for Biotechnology Information
nr	non-redundant
ORFs	open reading frames
PFU	plaque-forming unit
PhoH	phosphate starvation-inducible protein
RO medium	rich organic medium
SM	storage medium
TA	Type II toxin-antitoxin
TCT	serine
TDH	heat-resistant direct hemolysin
TEM	transmission electron microscopy
tRNA	transfer RNA
UVDE	putative UV DNA damage repair endonuclease
V. parahaemolyticus	*Vibrio parahaemolyticus*
vConTACT2	Viral CONTigs Automatic Clustering and Taxonomy v.2.0
VFDB	Virulence Factor Database
VICTOR	Virus Classification and Tree Building Online Resource
VIRIDIC	Virus Inter-genomic Distance Calculator

Supplementary Information

The online version contains supplementary material available at https://doi.org/10.1186/s12985-023-02036-9.

Supplementary Material 1: Table S1: Host range of phage R16F; **Table S2:** Predicted ORFs in the R16F genome; **Table S3:** Related phages identified by vCONTACT2 (score > 1)

Acknowledgements

We are grateful to Dr. Ruijie Ma and Dr. Long Wang for helpful advice on the manuscript.

Author contributions

R.Z., Y.Y., Y.C., Z.F., W.L., and K.S. performed the experiments and analyzed the data. Z.F. was responsible for phage isolation. Y.Y. prepared Figs. 1, 2, 3 and 4. Y.Y. and Y.C. prepared the supplementary material. Y.Y. and W.L. utilized software to process the genome data. Y.Y. and Y.C. performed formal analysis and wrote the main manuscript text. R.Z., Y.Y. and Y.C. reviewed and edited the manuscript. R.Z. and Y.Y. acquired the funding, organized and supervised the study. All authors reviewed the manuscript.

Funding

This study was supported by the National Key Research and Development Program of China (2020YFA0608300, 2021YFE0193000) and the National Natural Science Foundation of China (42106194).

Data availability

All data generated or analysed during this study are included in this published article and its supplementary information files.

Declarations

Ethics approval and consent to participate

Not applicable.

Consent for publication

Not applicable.

Competing interests

The authors declare that they have no competing interests.

Received: 18 December 2022 / Accepted: 11 April 2023
Published online: 01 May 2023

References

1. Ina-Salwany MY, Al-saari N, Mohamad A, Mursidi FA, Mohd-Aris A, Amal MNA, et al. Vibriosis in Fish: a review on Disease Development and Prevention. J Aquat Anim Health. 2019;31(1):3–22.
2. Mateus L, Costa L, Silva YJ, Pereira C, Cunha A, Almeida A. Efficiency of phage cocktails in the inactivation of *Vibrio* in aquaculture. Aquaculture. 2014;424–425:167–73.
3. de Souza Valente C, Wan AHL. *Vibrio* and major commercially important vibriosis diseases in decapod crustaceans. J Invertebr Pathol. 2021;181:107527.
4. Aguilera-Rivera D, Prieto-Davó A, Rodríguez-Fuentes G, Escalante-Herrera KS, Gaxiola G. A vibriosis outbreak in the Pacific white shrimp, *Litopenaeus vannamei* reared in biofloc and clear seawater. J Invertebr Pathol. 2019;167:107246.
5. Su YC, Liu C. *Vibrio parahaemolyticus*: a concern of seafood safety. Food Microbiol. 2007;24(6):549–58.

6. Parveen S, Hettiarachchi KA, Bowers JC, Jones JL, Tamplin ML, McKay R, et al. Seasonal distribution of total and pathogenic *Vibrio parahaemolyticus* in Chesapeake Bay oysters and waters. Int J Food Microbiol. 2008;128(2):354–61.
7. Letchumanan V, Loo K-Y, Woan-Fei Law J, Hei Wong S, Goh B-H, Ab Mutalib N-S, et al. Progress in Microbes and Molecular Biology *Vibrio parahaemolyticus*: the protagonist causing Foodborne Diseases. Prog Mol Biol Transl Sci. 2019;2(1):1.
8. Olumide A. Odeyem. Public health implications of microbial food safety and foodborne diseases in developing countries. Food Nutr Res. 2016;1:1–2.
9. Letchumanan V, Chan KG, Lee LH. *Vibrio parahaemolyticus*: A review on the pathogenesis, prevalence, and advance molecular identification techniques. Front Microbiol. 2014; 5.
10. Yang M, Liang Y, Huang S, Zhang J, Wang J, Chen H, et al. Isolation and characterization of the Novel Phages vB_VpS_BA3 and vB_VpS_CA8 for lysing *Vibrio parahaemolyticus*. Front Microbiol. 2020;11:1–13.
11. Lee LH, Mutalib NSA, Law JWF, Wong SH, Letchumanan V. Discovery on antibiotic resistance patterns of *Vibrio parahaemolyticus* in Selangor reveals carbapenemase producing *Vibrio parahaemolyticus* in marine and freshwater fish. Front Microbiol. 2018;9:1–13.
12. Letchumanan V, Loo K-Y, Law JW-F, Wong SH, Goh B-H, Ab Mutalib N-S, et al. *Vibrio parahaemolyticus*: the protagonist of foodborne diseases. Prog Microbes Mol Biol. 2019;2(1):1–8.
13. Tan CW, Rukayadi Y, Hasan H, Thung TY, Lee E, Rollon WD, et al. Prevalence and antibiotic resistance patterns of *Vibrio parahaemolyticus* isolated from different types of seafood in Selangor, Malaysia. Saudi J Biol Sci. 2020;27(6):1602–8.
14. Steward GF, Culley AI, Mueller JA, Wood-Charlson EM, Belcaid M, Poisson G. Are we missing half of the viruses in the ocean? ISME J. 2013;7(3):672–9.
15. Paez-Espino D, Eloe-Fadrosh EA, Pavlopoulos GA, Thomas AD, Huntemann M, Mikhailova N, et al. Uncovering Earth's virome. Nature. 2016;536(7617):425–30.
16. Weinbauer MG. Ecology of prokaryotic viruses. FEMS Microbiol Rev. 2004;28(2):127–81.
17. Suttle CA. Marine viruses - major players in the global ecosystem. Nat Rev Microbiol. 2007;5(10):801–12.
18. Gordillo Altamirano FL, Barr JJ. Phage therapy in the postantibiotic era. Clin Microbiol Rev. 2019;32(2):1–25.
19. Jun JW, Shin TH, Kim JH, Shin SP, Han JE, Heo GJ, et al. Bacteriophage therapy of a *Vibrio parahaemolyticus* infection caused by a multiple-antibiotic-resistant O3:K6 pandemic clinical strain. J Infect Dis. 2014;210(1):72–8.
20. Lomelí-Ortega CO, Martínez-Díaz SF. Phage therapy against *Vibrio parahaemolyticus* infection in the whiteleg shrimp (*Litopenaeus vannamei*) larvae. Aquaculture. 2014;434:208–11.
21. Wang Y, Barton M, Elliott L, Li X, Abraham S, O'Dea M, et al. Bacteriophage therapy for the control of *Vibrio harveyi* in greenlip abalone (*Haliotis laevigata*). Aquaculture. 2017;473:251–8.
22. Ren H, Li Z, Xu Y, Wang L, Li X. Protective effectiveness of feeding phage cocktails in controlling *Vibrio parahaemolyticus* infection of sea cucumber *Apostichopus japonicus*. Aquaculture. 2019;503:322–9.
23. Dubey S, Singh A, Kumar BTN, Singh NK, Tyagi A. Isolation and characterization of bacteriophages from Inland saline aquaculture environments to Control *Vibrio parahaemolyticus* contamination in shrimp. Indian J Microbiol. 2021;61(2):212–7.
24. Yang Y, Cai L, Ma R, Xu Y, Tong Y, Huang Y, et al. A novel roseosiphophage isolated from the oligotrophic South China Sea. Viruses. 2017;9(5):1–16.
25. Cai L, Ma R, Chen H, Yang Y, Jiao N, Zhang R. A newly isolated roseophage represents a distinct member of Siphoviridae family. Virol J. 2019;16(1):1–9.
26. Middelboe M, Chan AM, Bertelsen SK. Isolation and life cycle characterization of lytic viruses infecting heterotrophic bacteria and cyanobacteria.Man Aquat Viral Ecol. 2010;118–133.
27. Zerbino DR, Birney E, Velvet. Algorithms for de novo short read assembly using de bruijn graphs. Genome Res. 2008;18(5):821–9.
28. Garneau JR, Depardieu F, Fortier LC, Bikard D, Monot M, PhageTerm. A tool for fast and accurate determination of phage termini and packaging mechanism using next-generation sequencing data. Sci Rep. 2017;7(1):1–10.
29. Besemer J, Lomsadze A, Borodovsky M, GeneMarkS. A self-training method for prediction of gene starts in microbial genomes. Implications for finding sequence motifs in regulatory regions. Nucleic Acids Res. 2001;29(12):2607–18.
30. Lowe TM, Chan PP. tRNAscan-SE On-line: integrating search and context for analysis of transfer RNA genes. Nucleic Acids Res. 2016;44:W54–7.
31. Chen L, Yang J, Yu J, Yao Z, Sun L, Shen Y, et al. VFDB: a reference database for bacterial virulence factors. Nucleic Acids Res. 2005;33:325–8.
32. Alcock BP, Raphenya AR, Lau TTY, Tsang KK, Bouchard M, Edalatmand A, et al. CARD 2020: antibiotic resistome surveillance with the comprehensive antibiotic resistance database. Nucleic Acids Res. 2020;48:D517–25.
33. Jang HB, Bolduc B, Zablocki O, Kuhn JH, Roux S, Adriaenssens EM et al. Gene sharing networks to automate genome-based prokaryotic viral taxonomy. bioRxiv. 2019;231–238.
34. Meier-Kolthoff JP, Göker M. VICTOR: genome-based phylogeny and classification of prokaryotic viruses. Bioinformatics. 2017;33(21):3396–404.
35. Ma R, Lai J, Chen X, Wang L, Yang Y, Wei S et al. A Novel Phage Infecting *Alteromonas* Represents a Distinct Group of Siphophages Infecting Diverse Aquatic Copiotrophs.mSphere. 2021;6(3).
36. Meier-Kolthoff JP, Auch AF, Klenk HP, Göker M. Genome sequence-based species delimitation with confidence intervals and improved distance functions. BMC Bioinformatics. 2013;14.
37. Yu G. Using ggtree to visualize data on Tree-Like Structures. Curr Protoc Bioinformatics. 2020;69(1):1–18.
38. Farris JS. Estimating phylogenetic trees from Distance Matrices. Am Nat. 1972;106(951):645–68.
39. Moraru C, Varsani A, Kropinski AM. VIRIDIC—A novel tool to calculate the intergenomic similarities of prokaryote-infecting viruses. Viruses. 2020;12(11):1–10.
40. Cornelissen A. The T7-Related Pseudomonas putida Phage Q15 Displays Virion-Associated Biofilm Degradation Properties. 2010;6.
41. Lelchat F, Mocaer PY, Ojima T, Michel G, Sarthou G, Bucciarelli E, et al. Viral degradation of marine bacterial exopolysaccharides. FEMS Microbiol Ecol. 2019;95(7):1–11.
42. Schmelcher M, Loessner MJ. Bacteriophage endolysins: applications for food safety. Curr Opin Biotechnol. 2016;37:76–87.
43. Knecht LE, Veljkovic M, Fieseler L. Diversity and function of phage encoded depolymerases. Front Microbiol. 2020;10:1–16.
44. Cornelissen A, Ceyssens PJ, T'Syen J, van Praet H, Noben JP, Shaburova OV et al. The T7-related *Pseudomonas putida* phage φ15 displays virion-associated biofilm degradation properties.PLoS One. 2011;6(4).
45. Sasikala D, Srinivasan P. Characterization of potential lytic bacteriophage against *Vibrio alginolyticus* and its therapeutic implications on biofilm dispersal. Microb Pathog. 2016;101:24–35.
46. Majkowska-Skrobek G, Latka A, Berisio R, Squeglia F, Maciejewska B, Briers Y, et al. Phage-borne depolymerases decrease *Klebsiella pneumoniae* resistance to innate defense mechanisms. Front Microbiol. 2018;9:1–12.
47. Cao Y, Zhang Y, Lan W, Sun X. Characterization of vB_VpaP_MGD2, a newly isolated bacteriophage with biocontrol potential against multidrug-resistant *Vibrio parahaemolyticus*. Arch Virol. 2021;166(2):413–26.
48. Tan CW, Rukayadi Y, Hasan H, Abdul-Mutalib NA, Jambari NN, Hara H et al. Isolation and Characterization of Six *Vibrio parahaemolyticus* Lytic Bacteriophages from Seafood Samples.Front Microbiol. 2021;12.
49. Ding T, Sun H, Pan Q, Zhao F, Zhang Z, Ren H. Isolation and characterization of *Vibrio parahaemolyticus* bacteriophage vB_VpaS_PG07. Virus Res. 2020;286:198080.
50. Lal TM, Sano M, Ransangan J. Genome characterization of a novel vibriophage VpKK5 (*Siphoviridae*) specific to fish pathogenic strain of *Vibrio parahaemolyticus*. J Basic Microbiol. 2016;56(8):872–88.
51. Matamp N, Bhat SG. Genome characterization of novel lytic *myoviridae* bacteriophage ϕVP-1 enhances its applicability against MDR-biofilm-forming *Vibrio parahaemolyticus*. Arch Virol. 2020;165(2):387–96.
52. Thammatinna K, Egan MKE, Htoo HH, Khanna K, Sugie J, Nideffer JF, et al. A novel vibriophage exhibits inhibitory activity against host protein synthesis machinery. Sci Rep. 2020;10:1–14.
53. Yin Y, Ni P, Liu D, Yang S, Almeida A, Guo Q, et al. Bacteriophage potential against *Vibrio parahaemolyticus* biofilms. Food Control. 2019;98:156–63.
54. Zhang H, Yang Z, Zhou Y, Bao H, Wang R, Li T, et al. Application of a phage in decontaminating *Vibrio parahaemolyticus* in oysters. Int J Food Microbiol. 2018;275:24–31.
55. Abedon ST, Hyman P, Thomas C. Experimental examination of Bacteriophage latent-period evolution as a response to bacterial availability. Appl Environ Microbiol. 2003;69(12):7499–506.
56. Mäntynen S, Sundberg LR, Oksanen HM, Poranen MM. Half a century of research on membrane-containing bacteriophages: Bringing new concepts to modern virology.Viruses. 2019;11(1).
57. Turner D, Kropinski AM, Adriaenssens EM. A roadmap for genome-based phage taxonomy. Viruses. 2021;13(3):1–10.

58. Tom EF, Molineux IJ, Paff ML, Bull JJ. Experimental evolution of UV resistance in a phage. PeerJ. 2018;2018(7):1–20.
59. Paspaleva K, Moolenaar GF, Goosen N. Damage recognition by UV damage endonuclease from *Schizosaccharomyces pombe*. DNA Repair (Amst). 2009;8(5):600–11.
60. Yasui A. Alternative excision repair pathways.Cold Spring Harb Perspect Biol. 2013;5(6).
61. Warner HR, Persson ML, Bensen RJ, Mosbaugh DW, Linn S. Selective inhibition by harmane of the apurinic apyrimidinic endonuclease activity of phage T4-induced UV endonuclease. Nucleic Acids Res. 1981;9(22):6083–92.
62. Friedberg EC, King JJ. Dark repair of ultraviolet-irradiated deoxyribonucleic acid by bacteriophage T4: purification and characterization of a dimer-specific phage-induced endonuclease. J Bacteriol. 1971;106(2):500–7.
63. Friedberg EC, Walker GC, Siede W. DNA repair and mutagenesis. Washington, DC: ASM Press; 1995.
64. Lloyd RS, van Houten B. In DNA repair mechanisms: Impact on Human Diseases and Cancer. In: Vos JM, editor. DNA damage recognition. Austin: Biomedical Publishers; 1995. pp. 25–66.
65. Sancar A. DNA excision repair. Annu Rev Biochem. 1996;65:43–81.
66. Goosen N, Moolenaar GF. Role of ATP hydrolysis by UvrA and UvrB during nucleotide excision repair. Res Microbiol. 2001;152:401–9.
67. Truglio JJ, Rhau B, Croteau DL, Wang L, Skorvaga M, Karakas E, et al. Structural insights into the first incision reaction during nucleotide excision repair. EMBO J. 2005;24(5):885–94.
68. Fraikin N, Goormaghtigh F, Melderena L, Van. Type II Toxin-Antitoxin Systems: Evolution and Revolutions.J Bacteriol. 2020.
69. Makarova KS, Grishin NV, Koonin EV. The HicAB cassette, a putative novel, RNA-targeting toxin-antitoxin system in archaea and bacteria. Bioinformatics. 2006;22(21):2581–4.
70. Makarova KS, Wolf YI, Koonin EV. Comprehensive comparative-genomic analysis of Type 2 toxin-antitoxin systems and related mobile stress response systems in prokaryotes.Biol Direct. 2009;4.
71. Zhang S-P, Wang Q, Quan S-W, Yu X-Q, Wang Y, Guo D-D, et al. Type II toxin–antitoxin system in bacteria: activation, function, and mode of action. Biophys Rep. 2020;6:68–79.
72. Daimon Y, Narita SI, Akiyama Y. Activation of toxin-antitoxin system toxins suppresses lethality caused by the loss of σE in *Escherichia coli*. J Bacteriol. 2015;197(14):2316–24.
73. Butt A, Higman VA, Williams C, Crump MP, Hemsley CM, Harmer N, et al. The HicA toxin from *Burkholderia pseudomallei* has a role in persister cell formation. Biochem J. 2014;459(2):333–44.
74. Tang F, Bossers A, Harders F, Lu C, Smith H. Comparative genomic analysis of twelve *Streptococcus suis* (pro)phages. Genomics. 2013;101(6):336–44.
75. Niu YD, Cook SR, Wang J, Klima CL, Hsu YH, Kropinski AM et al. Comparative analysis of multiple inducible phages from *Mannheimia haemolytica*.BMC Microbiol. 2015;15(1).
76. Turner D, Ackermann HW, Kropinski AM, Lavigne R, Sutton JM, Reynolds DM. Comparative analysis of 37 *Acinetobacter* bacteriophages. Viruses. 2018;10(1):1–25.
77. Song S, Wood TK. A primary physiological role of Toxin/Antitoxin Systems is phage inhibition. Front Microbiol. 2020;11:1–7.
78. Byers DM, Gong H. Cover Image Acyl carrier protein: structure-function relationships in a conserved multifunctional protein family. Biochem Cell Biol. 2007;85(6):649–62.
79. Lu L, Cai L, Jiao N, Zhang R. Isolation and characterization of the first phage infecting ecologically important marine bacteria *Erythrobacter*. Virol J. 2017;14(1):1–15.
80. Forcone K, Coutinho FH, Cavalcanti GS, Silveira CB. Prophage genomics and ecology in the family *Rhodobacteraceae*.Microorganisms. 2021;9(6).
81. Torriani A, Ludtke DN. The molecular biology of bacterial growth. Boston: Jones and Bantell Publishers; 1985. pp. 224–42.
82. Wanner BL, Chang BD. The phoBR operon in *Escherichia coli* K-12. J Bacteriol. 1987;169(12):5569–74.
83. Kim SK, Makino K, Amemura M, Shinagawa H, Nakata A. Molecular analysis of the phoH gene, belonging to the phosphate regulon in *Escherichia coli*. J Bacteriol. 1993;175(5):1316–24.
84. Maina AN, Mwaura FB, Jumba M, Kiefts K, El-Din HTN, Aziz RK. Novel PhoH-encoding vibriophages with lytic activity against environmental *Vibrio* strains. Arch Microbiol. 2021;203:5321–31.
85. Miller ES, Heidelberg JF, Eisen JA, Nelson WC, Durkin AS, Ciecko A, et al. Complete genome sequence of the broad-host-range vibriophage KVP40: comparative genomics of a T4-related bacteriophage. J Bacteriol. 2003;185(17):5220–33.
86. Baudoux AC, Hendrix RW, Lander GC, Bailly X, Podell S, Paillard C, et al. Genomic and functional analysis of *Vibrio* phage SIO-2 reveals novel insights into ecology and evolution of marine siphoviruses. Environ Microbiol. 2012;14(8):2071–86.
87. Rong C, Zhou K, Li S, Xiao K, Xu Y, Zhang R et al. Isolation and Characterization of a Novel Cyanophage Encoding Multiple Auxiliary Metabolic Genes.Viruses. 2022;14(5).
88. Hatfull GF, Dedrick RM, Schooley RT. Phage therapy for antibiotic-resistant bacterial infections. Annu Rev Med. 2022;73:197–211.
89. Loessner MJ. Bacteriophage endolysins - current state of research and applications. Curr Opin Microbiol. 2005;8(4):480–7.
90. Pires DP, Oliveira H, Melo LDR, Sillankorva S, Azeredo J. Bacteriophage-encoded depolymerases: their diversity and biotechnological applications. Appl Microbiol Biotechnol. 2016;100(5):2141–51.
91. Wang W, Li M, Lin H, Wang J, Mao X. The *Vibrio parahaemolyticus*-infecting bacteriophage qdvp001: genome sequence and endolysin with a modular structure. Arch Virol. 2016;161(10):2645–52.

Publisher's Note